# Limiting Behaviour in Parameter Optimal Iterative Learning Control

D.H.Owens, M. Tomás-Rodríguez and J.J.Hatönen.
*ACSE DEPARTMENT. The Sheffield University.*
*Mappin Street. Sheffield. S1 3JD. United Kingdom.*
*d.h.owens@sheffield.ac.uk*

***Abstract*— This paper analyses the concept of *Limit Set* in Iterative Learning Control. The authors investigate the existence of *stable* and *unstable* parts of Limit Set and demonstrate that there will often exist in practice. This is illustrate via a 2-dimensional example where the convergence of the learning algorithm is analyzed from the error's dynamical behaviour. These ideas are extended to $N$-dimensional cases by analogy and example.**

Learning Control, Iterative systems, Optimization, Nonlinear systems.

## I. INTRODUCTION

Iterative learning control is a technique to control systems operating in a repetitive mode with the additional requirement that a specified output trajectory $r(t)$ defined over a finite time interval $[0, T]$ is followed to high precision. There are numerous examples of such systems including robot manipulators that are required to repeat a given task to a high precision. The main idea of iterative learning control is to use information from previous executions of the task in order to improve performance from trial to trial in the sense that the tracking error is sequentially reduced [1], this is: $Lim_{k\to\infty}||e_k|| = 0$.

Many approaches to ILC have been presented in past: A source of work up to 1993 is Moore [2] and the relevant cited references, and for more recent work the especial issue [3] together with conference papers and workshops. The ILC algorithm used in this paper, uses parameter optimization through a quadratic performance index as a method to establish the iterative learning control law. With this algorithm, monotonic convergence of the error to zero is guaranteed if the original system is a discrete-time LTI system and satisfies a positivity condition [4].

In the case of nonpositive definite plants, the required results of monotonic convergence to zero are not guaranteed. This anomalous behavior that will be analyzed in this paper and linked to @stair-like@ convergence behavior where periods of slow convergence over several iterations are followed by rapid convergence. this can happen several times in an iterative sequence.

The structure of the paper is as follows: In section 2 the ILC algorithm for a generic discrete time systems is proposed, the concept of *Limit Set* is introduced. Section 3 presents the concept of *stability* and *instability* of the limit set. A 2-Dimensional example is presented. In section 4 the phase-plane analysis for the previous example is carried out. Section 5 extends the ideas here exposed to the $N$-dimensional cases. Section 6 contains some conclusions and proposes future work directions.

## II. A BASIC ALGORITHM

Given the system:

$$x(t+1) = Ax(t) + Bu(t), \quad y(t) = Cx(t) \tag{1}$$

where the state $x(\cdot) \in R^n$, output $y(\cdot) \in R$, input $u(\cdot) \in R$ and $x(0) = x_0$. The operators $A$, $B$ and $C$ are matrices of appropriate dimensions. It will be assumed for simplicity that $CB \neq 0$ and the system (1) is controllable and observable. The idea is to find an iterative control law $u_{k+1} = f(u_k, u_{k-1}, \cdots, e_{k+1}, e_k, \cdots, e_{k-s})$ so that

$$Lim_{k\to\infty}||e_k|| = 0, \quad Lim_{k\to\infty}||u_k - u^*|| = 0$$

where $u_k = [u_k(0), u_k(1), \cdots, u_k(T)]^T$, $y_k = [y_k(0), y_k(1), \cdots, y_k(T)]^T$, $e_k = [r(0) - y_k(0), r(1) - y_k(1), \cdots, r(T) - y_k(T)]^T$, $||\cdot||$ is a suitable norm and $k$ is the trial index. Adopting the simple feedforward control law as in [4]:

$$u_{k+1}(t) = u_k(t) + \beta_{k+1}e_k(t+1) \tag{2}$$

where $\beta_{k+1}$ is a scalar gain parameter that will vary at each trial, it could be time-varied according to $\beta_{k+1}(t)$ where $t \in [0, T]$ and $h = \frac{T}{N}$.

In order to obtain the control input $u_{k+1}$ on the $(k+1)^{th}$ trial, at the end of each trial $k$, $\beta_{k+1}$ is selected to be the solution of the quadratic optimization problem:

$$\beta_{k+1} = min_{u_{k+1}}\left(J_{k+1}(\beta_{k+1})\right) \tag{3}$$
$$e_{k+1} = r - y_{k+1}, \quad y_{k+1} = Gu_{k+1}$$

where $G$ is a lower triangular matrix which elements are given by the Markov parameters of the plant, $G_{ij} = CA^{i-j}B$, (see[2]) and the performance index $J(\beta_{k+1})$ is defined as:

$$J(\beta_{k+1}) = ||e_{k+1}||^2 + w\beta_{k+1}^2 \tag{4}$$

and $w \geq 0$.

It is to be noted that the first term of (4) is designed to keep the tracking error small at each iteration. The second term of (4) tries to keep the magnitude of $\beta_{k+1}$ small, resulting in a more cautious and robust algorithm.

Using the updating law (2) and $e = r - Gu$ the tracking error update relation is of the form:

$$J(\beta_{k+1}) = ||e_{k+1}||^2 + w\beta_{k+1}^2 = ||(I - \beta_{k+1}G)e_k||^2 + w\beta_{k+1}^2$$
$$= ||e_k||^2 - \beta_{k+1}e_k^T(G + G^T)e_k + \beta_{k+1}^2||Ge_k||^2 + w\beta_{k+1}$$

Minimizing with respect $\beta_{k+1}$ gives:

$$\beta_{k+1} = \frac{< e_k, Ge_k >}{w + ||Ge_k||^2} \quad (5)$$

where $< \cdot, \cdot >$ is the chosen inner product and from (3) the error at each trial $k$ is given by the nonlinear iteration:

$$e_{k+1} = [I - \beta_{k+1}G]e_k \quad (6)$$

*Proposition 1:* The error $e_k$ decreases monotonically, $||e_{k+1}(\cdot)|| \leq ||e_k(\cdot)||$ with equality iff $\beta_{k+1} = 0$.

*Proposition 2:* $Lim_{k\to\infty}e_k = 0$ if $G + G^T > 0$ or $G + G^T < 0$.

At this point it is necessary to introduce the concept of *Limit Set*, $S_\infty$, as the set of all the possible values the error can converge to:

$$S_\infty = [e_\infty : e_\infty^T(G + G^T)e_\infty = 0, \quad (e_\infty^T G e_\infty = 0)] \quad (7)$$

This set is [0] iff $G + G^T > 0$ or $G + G^T < 0$.
In the next section, the dynamics of the limit set are going to be studied in the sense that its stability properties will be under discussion. A practical 2-dimensional example will be presented to illustrate the main ideas.

## III. LIMIT SETS

### A. Overview

As introduced in 2, $S_\infty$ denotes all possible cluster points of the ILC algorithm. In this section its dynamics are going to be studied from the stability point of view, defining the concept of *stability-instability* for the limit set.
The limit set $S_\infty \neq 0$, iff $G+G^T$ is not sign definite, this is, the limit set contains $e_\infty \neq 0$ if $G+G^T$ is not sign definite. In the case of $e_0 \in S_\infty$ then $e_k = e_0\ \forall k$ and then , the limit set $S_\infty$ can be thought as the set of equilibrium points of the ILC algorithm regarded as a dynamical system.
One might expect such *equilibria* to have stability properties , just as discrete dynamical systems do. In fact these dynamics can be found presenting a "stair"-like behavior as appears in fig.(1).

The apparent convergence (plateau) followed by further dynamics and a seconds phase of convergence, suggest a complex behavior of the limit set. The purpose of this paper is to explore this complex behavior by regarding the algorithm as a dynamical system. It is shown that some parts of the limit set denoted by

$$e_\infty^T(G + G^T)Ge_\infty > 0, \quad e_\infty^T(G + G^T)e_\infty = 0$$

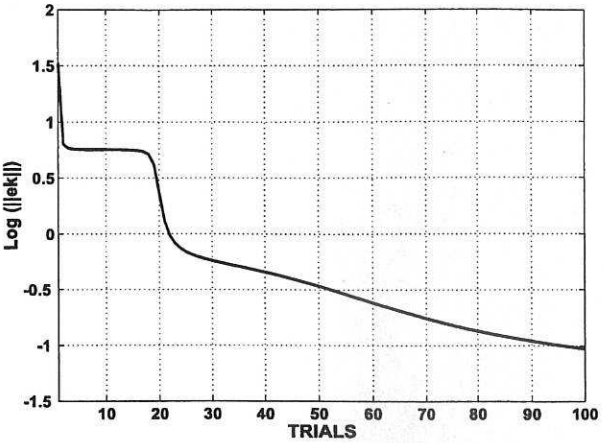


Fig. 1. Log$||e_k||$ for a generic system

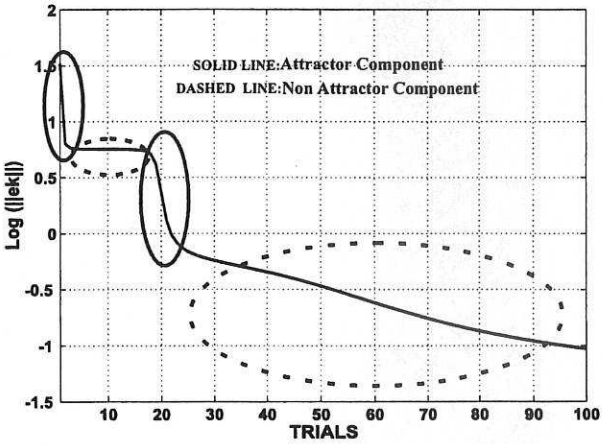


Fig. 2. Different regions of attraction in the $S_\infty$

attract trajectories, whilst the parts of the limit set where

$$e_\infty^T(G + G^T)Ge_\infty < 0$$

repel trajectories.
This section provides the detailed background to these statements and illustrates the graphical form of the conditions using the 2-D case. Note, that the components of $S_\infty$ where $e_\infty^T(G + G^T)Ge_\infty = 0$ are not studied as these dynamics are far more complex, this will be addressed in future works.
The generalization of these ideas to the $N$-dimensional case will be presented in the next section.
Recalling the definition of Limit Set as in (7), intuitively (see fig.2), any $e_k$ close to an attracting component, converges to a point $e_\infty$ in $S_\infty$. In the same way, if $e_k$ is near a repelling component of the limit set, $e_k$ moves away from $S_\infty$.

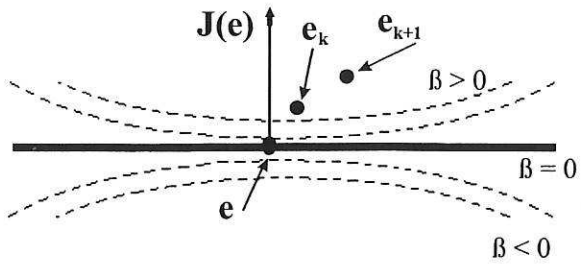


Fig. 3. Level curves for $\beta$

*B. Analysis*

The definition of limit set has been given in previous section and its analogy with a discrete time system has been addressed in the sense that the limit set presents a dynamical behavior consisting of attracting and repelling parts. In this section, the mathematical analysis of this behavior is going to be studied and a 2-dimensional example will be presented. It must be noted that the iterative maps are of the form:

$$\begin{pmatrix} e_k \\ \beta_{k+1} \end{pmatrix} \rightarrow \begin{pmatrix} e_{k+1} \\ \beta_{k+2} \end{pmatrix} \tag{8}$$

with equilibrium points (see [4]):

$$\begin{pmatrix} e_\infty \\ \beta_\infty \end{pmatrix}; \quad \beta_\infty = 0, \quad e_\infty^T G e_\infty = e_\infty^T (G + G^T) e_\infty = 0 \tag{9}$$

The task in here is to analyze the dynamics of the $S_\infty$ via the study of the dynamics of $\beta$, this is, by studying the level curves of $\beta = constant$ in $R^n$ (fig.3). The intuitive geometric condition for stability will be that $e_k$ moves towards the set $S_\infty$.
In order to simplify the analysis, note that those parts of $S_\infty$ that attract trajectories close to $S_\infty$ satisfy:

$$(\beta_{k+1} - \beta_k)\beta_k < 0$$

and repel trajectories if $(\beta_{k+1} - \beta_k)\beta_k > 0$.

From a geometric point of view, this can be summarized as follows:

*Proposition 3:* Close to the point $e_\infty \in S_\infty$,

$$\beta_k(\beta_{k+1} - \beta_k) > 0, \quad iff \quad e_\infty^T (G + G^T) G e_\infty < 0.$$

*Proof:*

$$\beta_{k+1} - \beta_k = \delta\beta \sim J(e_k)^T \delta_k,$$

where $J$ is the Jacobian and from (6), $e_{k+1} = e_k - \beta_{k+1} G e_k$.

Therefore,

$$\delta\beta \sim -J^T(e_k)\beta_{k+1} G e_k = -\beta_{k+1} e_k^T (G + G^T) G e_k$$

i.e.: $\beta_{k+1}\delta\beta = -\beta_{k+1}^2 e_k^T (G + G^T) G e_k$.

*Proposition 4:* Close to the point $e_\infty \in S_\infty$,

$$\beta_k(\beta_{k+1} - \beta_k) < 0, \quad iff \quad e_\infty^T (G + G^T) G e_\infty > 0.$$

*Proof: similar to proof above.*

These results have direct interpretation in terms of the stability properties of the components of $S_\infty$. For example,

*Proposition 5:* The points of the $S_\infty$ $(e : e^T G e = 0)$ for which $e^T(G + G^T)Ge < 0$ is satisfied, are non-attracting points.

In order to throw light at the nature of these conditions, consider the case of 2-dimensional matrix $G$:

$$G = \begin{pmatrix} 1 & 0 \\ \alpha & 1 \end{pmatrix}, \quad G + G^T = \begin{pmatrix} 2 & \alpha \\ \alpha & 2 \end{pmatrix} \tag{10}$$

with eigenvalues of $G + G^T$ at $\lambda = 2 \pm \alpha$ and eigenvectors $v_1 = (1,1)^T, v_2 = (-1,1)^T$. The eigenvalues and eigenvectors of $G^T + G$ need to be studied in order to analyze the dynamics of the $S_\infty$:

- $G + G^T > 0$ iff $\alpha^2 < 4$
- $(G + G^T)$ singular iff $\alpha \pm 2$
- $(G + G^T)$ sign-indefinite iff $\alpha^2 > 4$

Represented in the orthogonal eigenbasis of $(G + G^T)$, $e^T(G + G^T)e = 0$ is just:

$$e = \left( \sqrt{\alpha - 2} \begin{pmatrix} 1 \\ 1 \end{pmatrix} \pm \sqrt{\alpha + 2} \begin{pmatrix} -1 \\ 1 \end{pmatrix} \right) \cdot \gamma, \quad \gamma \in R. \tag{11}$$

where $\gamma$ is arbitrary.
In the case of $\alpha > 2$, there are two branches of the $S_\infty$ (stable and unstable, $S^-$ and $S^+$ respectively) which can be seen in fig.(4) and correspond to the different values $\pm$ of (11). It is seen that $S^+$ yields negative values and $S^-$ yields positive values, i.e.: the component $S^+$ of $S_\infty$ repels solutions whilst $S^-$ attracts solutions:

This is confirmed by evaluating $e^T(G^T + G)Ge$,

$$e^T(G^T + G)Ge = \left(2\alpha(\alpha^2 - 4) \pm 2\alpha^2\sqrt{\alpha^2 - 4}\right) \cdot \gamma^2$$

which is negative on $S^+$ and positive on $S^-$ if $\alpha > 2$. As a consequence, it is expected that almost all errors $e_k$ to converge towards the attracting parts of the $S_\infty$,i.e.:

$$Limit_{k \to \infty} e_k \in S^-.$$

for almost all $e_0 \in R^2$.
In order to support this idea of the sensitivity to the choice of initial error, $e_0$, consider the $G$ matrix with $\alpha = 3$:

$$G = \begin{pmatrix} 1 & 0 \\ \alpha & 1 \end{pmatrix}$$

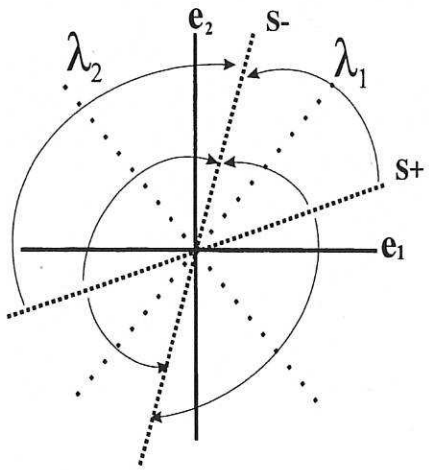


Fig. 4. $S_\infty$ components $S-$ and $S+$

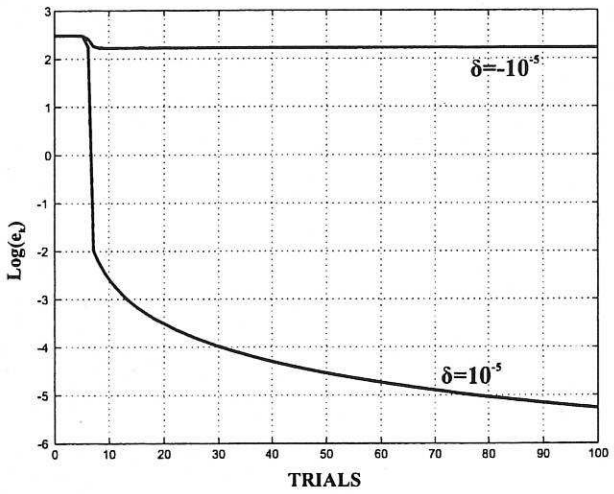


Fig. 5. $\text{Log}(||e_k||^2)$ with $+0.0001$ and $-0.0001$ displacement from $e_{0x}$

In this case the $S_\infty$ is parametrised:

$$e = \left(\sqrt{\alpha-2}\begin{pmatrix}1\\-1\end{pmatrix} \pm \sqrt{\alpha+2}\begin{pmatrix}1\\1\end{pmatrix}\right)\cdot\gamma, \quad \gamma \in R.$$

Taking the initial value of the error $e_0 \in S^+$ to be the pair $(1-\sqrt{5}\pm\delta, 1+\sqrt{5})$ where a small displacement $\delta = 10^{-5}$ from the point $(1-\sqrt{5}, 1+\sqrt{5})$ is applied, it can be seen in fig.(5) the different performance of the norm of the error: In the case of a negative perturbation, the error $e_0$ achieves a stationary value after approximately 10 iterations, whilst in the case of a positive perturbation, it decreases abruptly and then continues to decrease but at a slower rate. The difference in magnitude in the two cases is very large.

The great difference in performances indicates great sensitivity close to the unstable component $S^+$ of $S_\infty$. The final values of $\text{Log}(||e_k||^2)$ depend on the displacement $\delta$ from the initial $e_0$. That is, the convergence properties depend on the distance of the initial error from the stable part of the limit set, $S^+$.

If now $\delta$ is varied using the values $\delta = 0.1, 0.01, 0.00001$, it can be seen in fig. (6) that the smaller the perturbation, the greater the tendency of the $||e_k||$ to exhibit the "stair-like" properties seen in fig.(1). It is therefore seen that "stair-like" behaviors can occur and will tend to occur at points near the unstable component of the limit set.

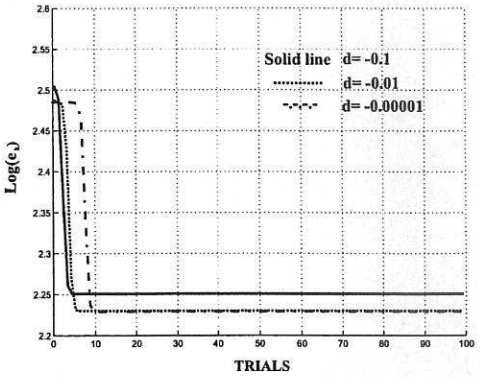


Fig. 6. $\text{Log}(||e_k||^2)$ with different displacements from $e_{0x}$

In practical terms this may leed to problems in differentiating between final or temporary convergence in performance. The next section looks at the previous example in terms of exact trajectories in $R^2$.

## IV. Phase-Plane Analysis

In this section, the phase-plane dynamics of (1) in $R^2$ are analyzed and the detailed behavior of the previous example is studied.

Take the matrix $G$ to be as in (10), with $\alpha = 3$ and $e_0 = (1-\sqrt{5}, 1+\sqrt{5}) \in S^+$ perturbed as $e_0 = (1-\sqrt{5}\pm\delta, 1+\sqrt{5})$. Two different cases are going to be studied; On the first case, the initial error is $e_0 = (1-\sqrt{5}-\delta, 1+\sqrt{5})$, and in the second case, $e_0 = (1-\sqrt{5}+\delta, 1+\sqrt{5})$, with $\delta = 10^{-5}$. The different movements of the ILC trajectories from $S^+$ to $S^-$ can be seen in fig.(7):

The speed of convergence is indicated by plotting $||e_{k+1} - e_k||$ at each trial $k$ for both cases.

- $1^{st}$ Case: $\delta = -10^{-5}$. Starting from the given $e_0$ with $Log(||e_0||^2) = 2.4849$, after 100 iterations, the error reaches the point $e_{100} = (-2.8479, 1.0878) \in S^-$, such that $Log(||e_{100}||^2) = 2.2282$ as appears in fig.(8) is smaller. It can be seen too, how the dynamics of the system, $||e_k||$, $\beta_k$, $||e_{k+1} - e_k||$ change at each trial.
- $2^{nd}$ Case: $\delta = 10^{-5}$. In this case, $e_{100} = (0.1209, -0.0461) \in S^-$, and it can seen in fig.(9) that the final value of $Log||e_100||^2 = -4.0903$.

In both cases it is seen that rapid movements of $e_k$ are associated with rapid movements in $\beta_k$ and $||e_{k+1} - e_k||$.

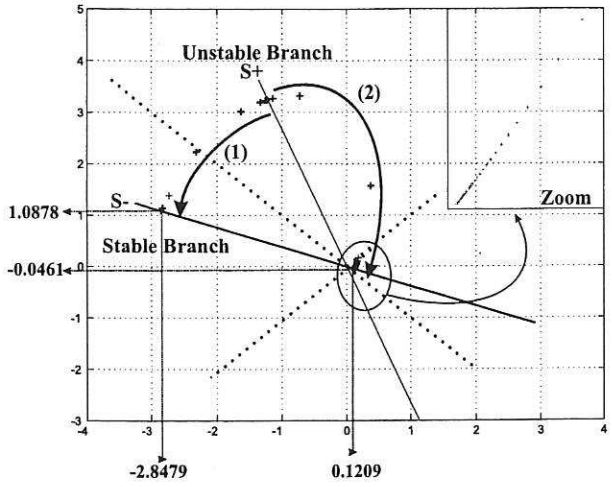


Fig. 7. Phase-plane trajectories for two different initial errors $e_0 \in S^+$

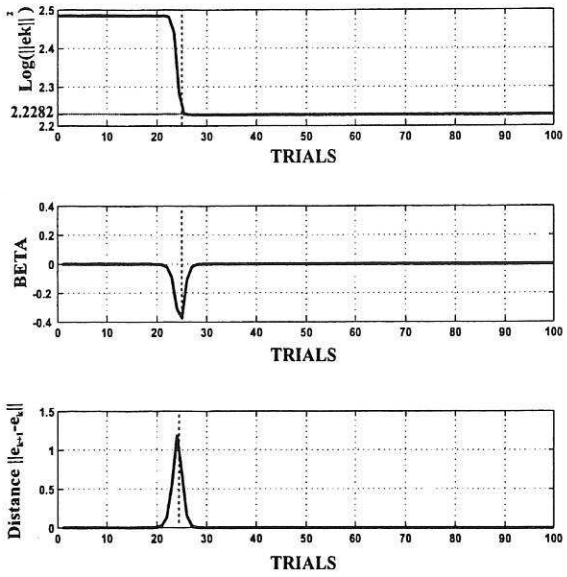


Fig. 8. *a*), $Log(||e_k||^2)$, *b*) Beta, *c*) Distance $||e_{k+1} - e_k||$

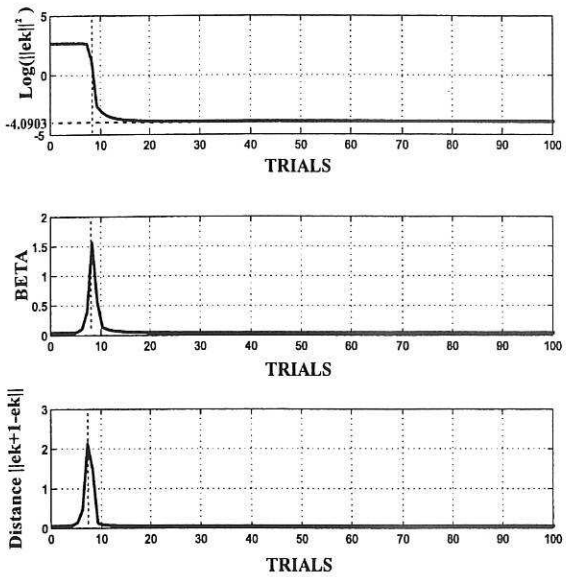


Fig. 9. *a*), $Log(||e_k||^2)$, *b*) Beta, *c*) Distance $||e_{k+1} - e_k||$

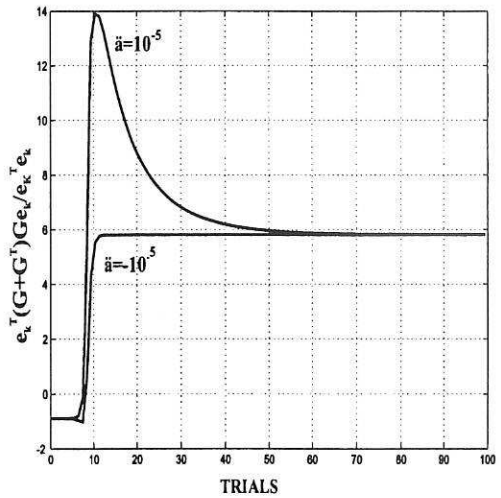


Fig. 10. $\frac{e_k^T(G+G^T)Ge_k}{e_k^T e_k}$ for different $e_0$.

Finally, the movement from the unstable $S^+$ to the stable $S^-$ region is seen in fig.(10) that plots the normalized quantity $\frac{e_k^T(G+G^T)Ge_k}{e_k^T e_k}$, starting off negative but converging to positive values.

## V. Generalization to $N$-Dimensional Cases

In this section, the $N$-dimensional case will be considered in a similar manner as in previous section for the 2-dimensional example. this is done using a nonpositive plant of the form, for example;

$$G(s) = \frac{1}{(s+1)^2} \tag{12}$$

the state space model in this case is defined by the following matrices:

$$A = \begin{pmatrix} -2 & -1 \\ 1 & 0 \end{pmatrix}, \quad B = \begin{pmatrix} 1 \\ 0 \end{pmatrix}, \quad C = (0, \quad 1) \tag{13}$$

Converting it into a discrete model using ZOH with time step $h = 0.1$, the next discrete time representation of (12) is obtained:

$$\Phi = \begin{pmatrix} 0.81435 & -0.090484 \\ 0.090484 & 0.99532 \end{pmatrix}, \quad \Delta = \begin{pmatrix} 0.090484 \\ 0.0046788 \end{pmatrix}$$
$$C = (0, \quad 1) \tag{14}$$

For this simulation the reference signal was chosen to be $r(t) = e^{\frac{t}{20}} sinwt$ over the time interval $t \in [0, 20]$ with a frequency of $w = 1$. The value of the parameter $W$ is

$W = 10^{-6}$ and $u_0 = 0$.
The eigenvalues of the 200x200 matrix $(G + G^T)$ are in the range of $(-0.2086, 1.8942)$, so this shows that $G + G^T$ is not a positive definite matrix and hence $S_\infty$ contains non-zero points in $R^{200}$- a high dimensional space.

Fig.(11) shows the evolution of the norm of the error and the evolution of $Q = \frac{e_k^T(G+G^T)Ge_k}{e_k^T e_k}$.

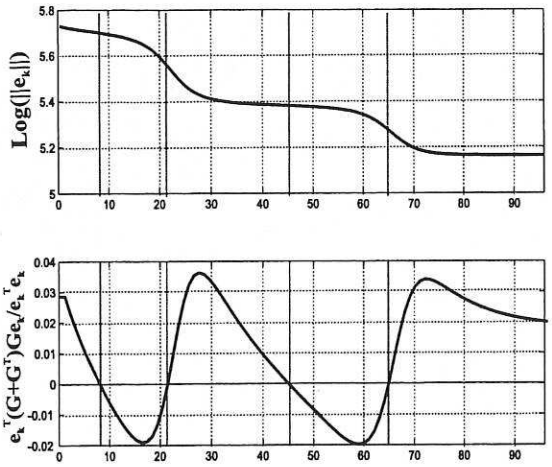


Fig. 11. Error and normalized $e_k^T(G + G^T)Ge_k$

It is clear that in this high dimension case the "stair-like" behavior of the norm of error appears in the same form as in fig.(1). Slow movement of the norm is associated with small values of $\beta_k$ and hence convergence of the error vector to $S_\infty$. The sign of $e(G + G^T)Ge^T$ varies taking both positive and negative values. In particular, it moves rapidly from negative to positive as the error norm reduces rapidly. This is consistent with the intuition that the algorithm is moving from a portion close to $S^+$ towards $S^-$.
Fig.(12) shows the evolution of the beta value $\beta_k$ and the evolution of the distance between two consecutive errors $||e_{k+1} - e_k||$. These dynamics are strongly correlated to the changes in the dynamics of $e_k$.

## VI. CONCLUSIONS AND FUTURE WORKS

In this paper, the concepts of Limit Set and its stability have been introduced. Experience in simulations suggests the existence of attracting and repelling components of the Limit Set. conditions for these properties have been derived in general and the existence of repelling components illustrated by a detailed 2-Dimensional example.
Altough the details are different, it is seen that the general conclusions deduced from the $N = 2$ example do throw light on more general high dimensional cases. The authors believe that the observed phenomena are typical of behaviours that will be met in all applications of parameter-optimal ILC. Further study of the properties of $S_\infty$, $S^+$ and $S^-$ are seen to be crucial to both theory and practice and will extend to

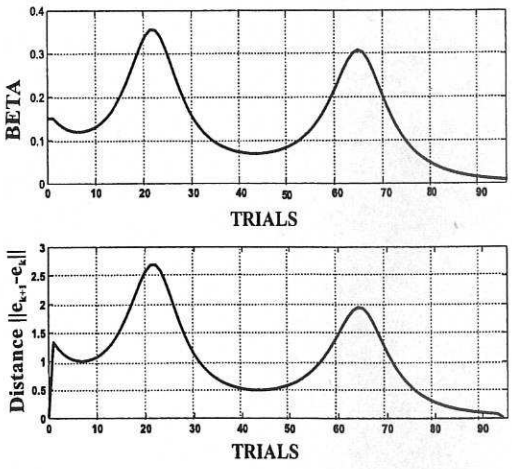


Fig. 12. $\beta_k$ and $||e_{k+1} - e_k||$

more general parameter-optimal ILC methods. Further work is hence desirable to understand the behaviour more clearly and to develop diagnostic tools to monitor and improve performance. Current work in Sheffield is addressing these issues.

## REFERENCES


[1] Arimoto, S., Kawamura, S. Miyazaki, F. Bettering operations and robot learning, *Journal of robotic systems*, vol. 1, 1984, pp 123-140.
[2] Moore, K., *Iterative learning control for deterministic systems*, Springer, London; 1993.
[3] Moore, K. Xu, J-K. *Special Issue of the international Journal of control on Iterative Learning Control*, 73(10); 2000.
[4] Hatönen, J.J., Owens, D.H., Feng,K. *Basis functions and Parameter Optimization in High-Order Iterative Learning Control*, in Third SIAM Conference on Applied Linear Algebra; 2003.